4954 *Macromolecules* **2010**, *43*, 4954–4960
DOI: 10.1021/ma100314z

Macromolecules
ARTICLE

Thermoplastic Elastomers with Composite Crystalline−Glassy Hard Domains and Single-Phase Melts

John P. Bishop and Richard A. Register*

Department of Chemical Engineering, Princeton University, Princeton, New Jersey 08544-5263

Received February 8, 2010; Revised Manuscript Received April 2, 2010

ABSTRACT: We report the synthesis and characterization of thermoplastic elastomers (TPEs) containing both crystalline and glassy hard segments, with the aim of capturing the mechanical properties of conventional all-amorphous triblock TPEs, while forming the solid-state structure by crystallization from a single-phase melt. To accomplish this, we used living ring-opening metathesis polymerization (ROMP) and subsequent hydrogenation to synthesize symmetric pentablock copolymers with the architecture crystalline−glassy−rubbery−glassy−crystalline. Analogous crystalline−rubbery−crystalline triblocks show a high initial modulus, yielding, and poor recovery, resulting from platelike crystalline hard blocks. By contrast, with the pentablock architecture and appropriate selection of block lengths, crystallization from a single-phase melt causes a layer rich in the glassy block to form around the crystallites, limiting their lateral growth and generating composite hard domains with both crystalline and glassy components. The pentablocks show the low initial modulus, strain-hardening behavior, and small permanent set desired for TPEs, while retaining an easily processed single-phase melt.

Introduction

An important class of thermoplastic elastomers (TPEs) are ABA triblock copolymers made up of a majority component rubbery mid-block (B) and minority component glassy end-blocks (A). The most common of these are styrenic block copolymers, where polystyrene serves as the end-blocks (typically 15−35 wt %) with the rubbery mid-block being a polydiene.[1] In these materials, repulsion between the polystyrene and polydiene blocks causes microphase separation; at room temperature, anchoring of the rubbery mid-block chains by the glassy end-blocks creates a physically cross-linked material exhibiting elastomeric behavior. In these types of TPEs where both the hard and soft blocks are amorphous, it is necessary to have a high degree of interblock incompatibility—not merely sufficient to achieve microphase separation, but strong enough to produce relatively pure domains so that the TPE exhibits a broad use temperature range. However, the high viscosities and elasticities of the microphase-separated melts have an adverse effect on the processability of the material.[2]

If instead the hard segments are crystalline, microphase separation can be driven by crystallization from a single-phase melt; strong interblock repulsion is not required. The use of crystalline end-blocks in TPEs can also confer solvent resistance to the material.[3] Indeed, there has been considerable research on ABA triblock copolymers containing crystalline end-blocks, where microphase separation is driven by crystallization from a single-phase melt; typically, these materials contain hydrogenated high 1,4-polybutadiene (hPBd) as the crystalline component and either a hydrogenated polyisoprene (poly(ethylene-*alt*-propylene), PEP) or a high vinyl (≥40%) hydrogenated polybutadiene (poly(ethylene-*ran*-butene), PEB) as the rubbery mid-block, all synthesized by anionic polymerization and subsequent hydrogenation.[3−6] Unfortunately, these semicrystalline TPEs were plagued by poor tensile strengths and/or high permanent sets relative to their amorphous counterparts due to irreversible yielding of the crystalline domains. Hotta et al. studied semicrystalline thermoplastic elastomers with isotactic polypropylene (iPP) hard blocks and regioirregular polypropylene (rPP) soft blocks.[7] An iPP−rPP−iPP triblock crystallized from a homogeneous melt showed excellent extensibility and permanent set but modest tensile strength. A symmetric pentablock containing an internal crystalline block, iPP−rPP−iPP−rPP−iPP, showed a single-phase melt and excellent extensibility and permanent set and a 4-fold higher tensile strength than the triblock. The authors attributed the increased strength to the effectiveness of the internal hard block in thwarting chain pullout; similar improvements in tensile strength with increasing number of blocks (up to 13) were demonstrated by Koo et al. in alternating hPBd−PEP multiblocks.[8] High extensibilities and low permanent sets have been demonstrated in multiblock copolymers of polyethylene and poly(ethylene-*ran*-octene)[9,10] made using Dow Chemical's "chain-shuttling" polymerization chemistry[11] when the hard block content is suitably low; these polymers contain 2−10 blocks per chain. These multiblock systems are reminiscent of segmented block copolymers such as thermoplastic poly(ether ester) elastomers, where the hard blocks are typically semicrystalline poly(tetramethylene terephthalate) and the soft blocks are typically poly(tetramethylene oxide).[12] These polymers normally have short block lengths (∼1000 g/mol), which result in homogeneous melts that are easily processed.[13] However, relatively high hard block contents are required to achieve hard blocks long enough to exhibit sufficiently high melting points, resulting in TPEs that have relatively high moduli and considerable permanent set. Indeed, balancing the competing requirements of low hard segment content (for elastomeric behavior), high number of blocks per chain (for good recovery), sufficient hard block molecular weight (for a sufficiently high melting point), and moderate total chain length (to ensure that even the single-phase melt remains tractable) is a challenge in such multiblock systems.

Here, we describe a different approach to generating TPEs with good recovery and single-phase melts by judiciously combining

*Corresponding author. E-mail: register@princeton.edu.

 Published on Web 05/07/2010

crystalline and glassy hard blocks. The goal is to incorporate the beneficial properties of both components: the superior tensile strength of a glassy block along with a solid-state structure formed by crystallization from a lower viscosity single-phase melt. Several groups have previously combined rubbery, glassy, and crystalline blocks in an effort to generate superior TPEs;[14−19] most commonly, these are ABC triblock copolymers,[14−16] where B is the majority rubbery component, A is glassy, and C is crystalline. While such materials do behave as TPEs, their mechanical properties are generally similar to all-amorphous ABA triblocks, with lower ultimate tensile strengths[14] and higher permanent sets following large deformations,[16] reflecting yielding of the crystalline C block. Moreover, for the A block to form effective physical cross-links, it must microphase-separate from the B and C blocks, so the processing advantages of a single-phase melt are not captured.

Very recently, Fleury and Bates[19] showed that TPE behavior can be achieved in an undecablock copolymer, where structure develops by crystallization from a single-phase melt; in this copolymer, the rubbery mid-block (50 wt %) is flanked by two pentablocks of the structure glassy−crystalline−glassy−crystalline−glassy. In the present work, we demonstrate that TPE behavior, including an easily processed single-phase melt and excellent recovery from deformation at room temperature, can be achieved using a relatively simple macromolecular architecture: pentablock copolymers with the architecture crystalline−glassy−rubbery−glassy−crystalline. With the appropriate selection of block lengths, crystallization from a single-phase melt causes a layer rich in the glassy block to form around the growing crystallites, restricting their lateral extent and connectivity and yielding a resilient elastomer.

Experimental Section

Materials. The monomers 5-hexylnorbornene (HN, racemic mixture of enantiomers, 77:23 mixture of *endo*:*exo*[20]) and methyltetracyclododecene (MTD, systematic name is 8-methyltetracyclo[4.4.0.$1^{2,5}$.$1^{7,10}$]dodec-3-ene; monomer is a 2:1 mixture of *endo*/*anti* and *exo*/*syn* isomers;[21] see Supporting Information) were obtained from Promerus. Norbornene (N) was obtained from Aldrich. Each monomer was dried over sodium, degassed by freeze−pump−thaw cycles, and vacuum transferred prior to use. Toluene was dried over sodium benzophenone ketyl or diphenylhexyllithium (adduct of butyllithium and diphenylethylene), degassed by freeze−pump−thaw cycles, and vacuum transferred prior to use. The "Schrock-type" initiator, 2,6-diisopropylphenylimidoneophylidenemolybdenum(VI) bis(*tert*-butoxide), was used as received from Strem Chemicals. The terminating agents benzaldehyde (Aldrich, 99.5+%, SureSeal) and isophthalaldehyde were used as received. For hydrogenation, a heterogeneous catalyst containing 5 wt % Pd^0 supported on $CaCO_3$ (Alfa Aesar) was used as received.

Polymerization. Living ring-opening metathesis polymerizations (ROMP) were conducted in toluene solution, in an Innovative Technologies System One glovebox with water and oxygen contents less than 1.0 ppm. Triblock copolymers were synthesized by sequential addition of three monomer charges (N, HN, N or MTD, HN, MTD) to an initiator solution in toluene, and the reaction was terminated with a 100-fold molar excess of benzaldehyde. For the pentablocks, half of the polymer was synthesized by sequential addition of three monomer charges (N, MTD, HN), followed by coupling the living PHN ends by terminating with a stoichiometric amount of isophthalaldehyde.[22,23] Prior to the addition of each monomer or isophthalaldehyde, a reaction aliquot was removed and terminated with a large excess of benzaldehyde for characterization. Reaction times were 30 min for N and MTD blocks and 60 min for HN blocks. The resulting copolymers were isolated by precipitating into methanol three times and vacuum-drying.

Hydrogenation. Polymers were dissolved in cyclohexane at 5 g/L; for the precursor to hPN−hPHN−hPN, an 80/20 mixture of cyclohexane/THF was used to speed dissolution. Hydrogenations were carried out in a 2 L Parr reactor at 500 psig H_2 and 100 °C using $Pd^0/CaCO_3$. Hydrogenation was continued until the *trans* C=C double bond stretch was undetectable by infrared spectroscopy, corresponding to >99.9% saturation.

Molecular Characterization. Gel permeation chromatography (GPC) in THF was used to characterize the molecular weight distribution of the soluble, unsaturated block copolymers prior to hydrogenation. In the case of the two hPMTD−hPHN−hPMTD triblocks, where the polymers were soluble in THF at room temperature both before and after hydrogenation, GPC was used to confirm that no degradation or other side reactions involving the backbone occurred during hydrogenation. The GPC system consists of two 30 cm Polymer Laboratories PLgel Mixed-C columns, a Waters 515 HPLC pump, and a Waters 410 differential refractometer. The GPC columns were calibrated with narrow-distribution polystyrene standards, and the resulting "polystyrene-equivalent" molecular weights were converted to their true values by dividing by the appropriate hydrodynamic correction factor[24] (r = 1.96 for PN, superseding our previous[20] value; r = 1.32 for PHN, and r = 1.07 for PMTD). Block copolymer compositions were determined by ^{1}H NMR in $CDCl_3$ on the soluble, unsaturated polymers; see Supporting Information for detailed procedures. The analyzed block copolymer compositions were always close to the target values (weight fractions within 0.5%). An hPMTD homopolymer (M_n = 123 kg/mol, PDI = 1.09) was synthesized analogously to the block copolymers and was used to generate all the hPTMD homopolymer physical property data reported herein.

Thermal, Mechanical, and Morphological Characterization. Differential scanning calorimetry (DSC) data were acquired with a Perkin-Elmer DSC-7, calibrated on heating with indium and tin, with a scan rate of 10 °C/min. Fractional degrees of crystallinity of the hPN blocks ($w_{c,hPN}$) were calculated from the melting enthalpies using the known hPN weight fractions in the block copolymers and taking 86 J/g as the heat of melting of perfectly crystalline hPN.[25] Densities at 23.0 ± 0.1 °C were measured in a methanol/ethylene glycol density gradient column (Techne DC-4), calibrated with glass floats. Steady-shear viscosity−shear rate curves at 180 and 200 °C were generated using a constant-stress rheometer (Anton Paar MCR-501). A 25 mm cone-and-plate fixture was used for all of the block copolymers except for hPMTD−hPHN−hPMTD-H, whose melt was too elastic to test in the cone-and-plate geometry. A 25 mm plate-and-plate fixture was used instead for this polymer, where the shear rate reported corresponds to the shear rate at the rim of the plate-and-plate fixture, and the viscosity reported is the torque-weighted average across the fixture. Room-temperature uniaxial tensile stress−strain curves were obtained with either an Instron model 1122 or 5865 at a cross-head speed of 2 in./min on ASTM D1708 dog bones (2−4 replicates) stamped at room temperature from sheets which were compression-molded at 180 °C (160 °C for hPN−hPHN−hPN). The standard deviation for the resulting Young's moduli (E) were within 5% of the mean, while the standard deviation for the tensile strength (σ_u) and breaking strain (ε_b) measurements were within 10% of the mean. For permanent set measurements, the polymers were stretched to 300% engineering strain, and the cross-head immediately reversed and returned to its initial position, all at a cross-head speed of 2 in./min. A caliper was used to measure the recovered length 10 min after the experiment, and the permanent set was calculated as a percentage of the original gauge length. Atomic force microscopy phase images were acquired with a Digital Instruments (now Veeco) Dimension 3000 AFM equipped with a Nanoscope IIIa controller, in tapping mode using Si tips (Veeco) resonating at 300 kHz. Specimens were prepared by spin-coating from a 2 wt % polymer solution in cyclohexane at 65 °C, onto a Si wafer at 3000 rpm,

to yield films ≈200 nm thick as determined by ellipsometry (Gaertner Scientific LS116S300). After spin-coating, films were heated on a digital hot plate to 140 °C for 10−15 min and then cooled to 65 °C to effect isothermal recrystallization of the material. Small-angle X-ray scattering (SAXS) patterns were acquired with an Anton-Paar compact Kratky camera equipped with a hot stage and an M. Braun OED-50 M position-sensitive detector. Data were corrected for detector sensitivity and positional linearity, empty beam scattering, and sample thickness and transmittance, placed on an absolute intensity scale via a polyethylene standard, and desmeared for slit length.[26] Intensities are presented against the magnitude of the momentum transfer vector $q = (4\pi/\lambda) \sin \theta$, where θ is half the scattering angle. Silver behenate ($d = 5.838$ nm) was used to calibrate the scattering angle.[27] For hPN-containing materials, samples were isothermally crystallized at elevated temperatures (10 °C above the peak crystallization temperature measured by DSC during cooling at 10 °C/min) until no further increase in SAXS intensity was observed (typically 2 h).

Results and Discussion

Living ring-opening metathesis polymerization (ROMP) and subsequent hydrogenation was employed to synthesize the TPEs reported herein. This synthesis method provides ready access to crystalline, glassy, and rubbery blocks: semicrystalline hydrogenated polynorbornene (hPN), a highly crystalline polymer with an equilibrium melting temperature $T_m^0 = 156$ °C;[28] hydrogenated poly(5-hexylnorbornene) (hPHN), a rubbery amorphous polymer with $T_g = -22$ °C;[20] and hydrogenated polymethyltetracyclododecene[29] (hPMTD), a glassy polymer with $T_g = 163$ °C, as measured herein by DSC. The high T_g of hPMTD allows for higher upper use temperatures than in conventional styrenic TPEs, especially at the modest end-block molecular weights typically employed. The chemical structures for each of these building blocks is shown in Figure 1, while the composition and molecular weight for each of the block copolymers are given in Table 1. The total hard block content (hPN + hPMTD) was kept at 20 wt % across the series to permit a direct comparison of the influence of crystalline vs glassy vs composite hard domains on mechanical properties. First we consider the melt and solid-state morphology of each of the materials, beginning with the triblock copolymers.

The SAXS pattern of hPMTD−hPHN−hPMTD-H (Figure 2a) at 200 °C shows a relatively narrow first-order peak indicating a microphase-separated structure. The minimum and maximum near 0.25 and 0.4 nm^{-1} result from the form factor[30] of cylindrical hPMTD domains; their positions are consistent with the position of the primary peak and the hPMTD volume fraction, confirming a cylindrical morphology. This SAXS pattern persists until at least 260 °C, the highest temperature employed; the pattern at room temperature (Figure 2a) is similar in shape to that in the melt, but with a reduced contrast resulting from the higher thermal expansion coefficient of rubbery hPHN vs glassy hPMTD (the density of hPMTD homopolymer at 23 °C was measured as 1.0078 g/cm^3 vs 0.9086 g/cm^3 for hPHN[20]). By contrast, the lower-molecular-weight hPMTD−hPHN−hPMTD-L showed a featureless SAXS pattern at all temperatures, implying a disordered melt, yet showed room-temperature stress−strain behavior characteristic of an elastomer (see Supporting Information). This implies that hPMTD−hPHN−hPMTD-L has an order−disorder transition between 200 °C and room temperature but that as soon as the hPMTD blocks aggregate, they immediately vitrify; recall that $T_g = 163$ °C for high-molecular-weight hPMTD.

Turning to the crystalline end-block material, the melt-phase pattern (140 °C) for hPN−hPHN−hPN (Figure 2b) shows no peaks, consistent with a single-phase melt. We calculate an electron density difference $\Delta\rho_e > 14$ e/nm^3 at 140 °C between the two components from the room temperature mass densities of hPN[28] and hPHN[20] along with the thermal expansion coefficients for hPN and hydrogenated polyethylidenenorbornene,[31] a polymer similar in structure to hPHN. This electron density difference

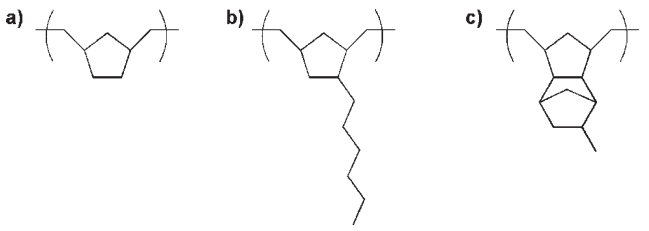

Figure 1. Repeat units for (a) hydrogenated polynorbornene (hPN), (b) hydrogenated polyhexylnorbornene (hPHN), and (c) hydrogenated polymethyltetracyclododecene (hPMTD).

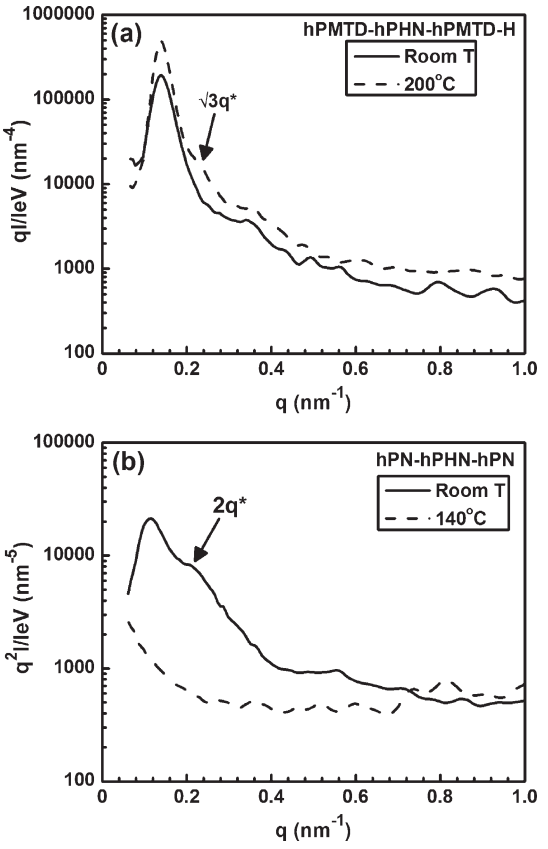

Figure 2. Melt and room-temperature SAXS patterns for (a) hPMTD−hPHN−hPMTD-H and (b) hPN−hPHN−hPN.

Table 1. ROMP TPE Molecular Characterization Data

polymer	M_n (kg/mol)	M_w/M_n	block lengths (kg/mol)	f_{hPN}	f_{hPMTD}
pentablock-10	193	1.09	10−10−153−10−10	0.10	0.10
pentablock-14	200	1.10	14−7−158−7−14	0.14	0.07
hPN−hPHN−hPN	128	1.05	13−102−13	0.20	
hPMTD−hPHN−hPMTD-H	250	1.09	25−200−25		0.20
hPMTD−hPHN−hPMTD-L	158	1.06	16−125−16		0.20

is more than sufficient to observe any microphase separation in the melt. Following isothermal crystallization at 75 °C and cooling to room temperature, the SAXS pattern shows a broad first-order peak at $q^* = 0.117$ nm^{-1} (Bragg spacing $d = 2\pi/q^* =$ 54 nm) and a clear second-order shoulder, indicating the expected crystallization-induced lamellar microstructure. The thickness of the hPN crystals can therefore be calculated as $t_c = \phi_c d$, where ϕ_c is the volume fraction of the hPN crystals in the block copolymer, calculated from the mass densities quoted and referenced above, and the $w_{c,hPN}$ determined by DSC; for hPN−hPHN−hPN, t_c is found to be 5.2 nm.

Taken together, these observations provide a rough guideline for the design of pentablocks with a single-phase melt. The interaction parameter between hPN and hPHN is unknown, but modest, since hPN−hPHN−hPN forms a single-phase melt at block molecular weights of 13−102−13 kg/mol. By contrast, hPMTD−hPHN−hPMTD-L is on the border of microphase separation at block molecular weights of 16−125−16 kg/mol. These observations suggest that pentablocks containing "hard" blocks (hPN + hPMTD) of 20 kg/mol total, and at least 50% hPN, should be homogeneous or at most weakly segregated. We synthesized two such pentablocks, both with rubbery hPHN center blocks of 155 ± 3 kg/mol: one with hard blocks of 10 kg/mol hPN and 10 kg/mol hPMTD (pentablock-10) and a second with a higher fraction of crystalline material, having hard blocks of 14 kg/mol hPN and 7 kg/mol hPMTD (pentablock-14). Unlike the triblock copolymers, which were synthesized using a sequential monomer charge for each block, the final synthesis step for both of the pentablocks was to couple the living ends using a difunctional terminating agent, isophthalaldehyde. Elution traces after each reaction step for pentablock-14 are shown in Figure 3, illustrating that only a small fraction of uncoupled triblock is present in the final product.

The melt SAXS patterns of pentablock-10 (Figure 4a) and pentablock-14 (Figure 4b) are featureless, reflecting the expected single-phase melts. Pentablock-10 and pentablock-14 were isothermally crystallized at 68 and 66 °C, respectively, and then slow-cooled to room temperature. The room-temperature SAXS pattern for pentablock-10 (Figure 4a) shows a broad first-order peak at $q^* = 0.093$ nm^{-1}, which corresponds to a Bragg spacing of 68 nm. The degree of crystallinity of the hPN blocks in pentablock-10 is quite low (15%, Table 2); assuming an alternating lamellar structure would lead to an unrealistically small value of 0.9 nm for the hPN crystal thickness. This is a clear indication that the hPN crystals in pentablock-10 are discontinuous, i.e., of very limited lateral extent, as the similar melting points (Table 2) of pentablock-10 (114 °C) and hPN−hPHN−hPN (120 °C) indicate a comparable crystal thickness for the two. The room-temperature SAXS pattern of pentablock-14 (Figure 4b) similarly shows a broad first-order peak at $q^* = 0.104$ nm^{-1} ($d = 60$ nm). Assuming an alternating lamellar microstructure, the crystallinity of the hPN blocks in pentablock-14 (54%) would lead to an hPN crystal thickness of 4.2 nm, slightly smaller than the value found for hPN−hPHN−hPN. However, as shown below by atomic force microscopy (AFM) and by mechanical testing, the hPN crystals in pentablock-14 are also substantially discontinuous.

To complement the SAXS patterns, real-space images of pentablock-14 were acquired by AFM. Figure 5a shows the AFM phase image immediately after spin-coating from cyclohexane into a 200 nm thick film. Bright (higher modulus) nodules are visible in a darker matrix; the Fourier transform of this image (Figure 5c) shows a peak at $q^* = 0.19$ nm^{-1}, indicating a characteristic spacing of ~33 nm. (The y-axis of the Fourier transform in Figure 5c was multiplied by q^2 simply to facilitate comparison with the SAXS

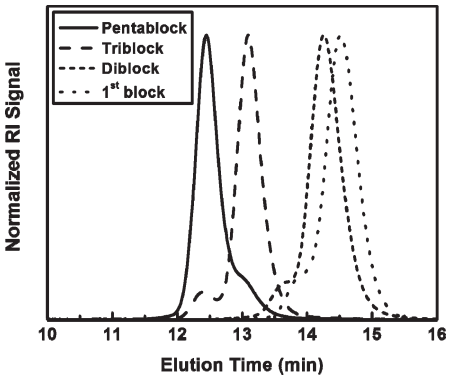

Figure 3. GPC elution traces after each reaction step in the ROMP synthesis of pentablock-14. The final reaction product (solid curve) contains primarily the pentablock, with only a small fraction of uncoupled triblock.

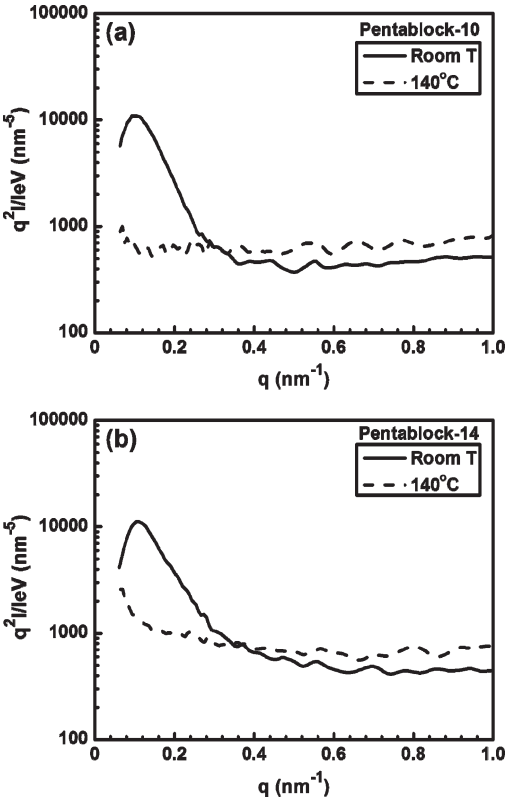

Figure 4. Melt and room-temperature SAXS patterns for (a) pentablock-10 and (b) pentablock-14.

Table 2. ROMP TPE Thermal and Molecular Characterization Data

polymer	T_g[a] (°C)	T_m (°C)	ΔH_m (J/g)	$w_{c,hPN}$[b]	E (MPa)	σ_u (MPa)	ε_b (%)	set[c] (%)
pentablock-10	−13	114	1.2	0.15	4.9	7.4	450	9
pentablock-14	−16	117	6.5	0.54	3.5	5.3	520	6
hPN−hPHN−hPN	−14	120	9.2	0.53	22	9.8	420	44
hPMTD−hPHN−hPMTD-H	−18				4.2	15	460	8

[a] Of rubbery phase. [b] Weight fraction crystallinity of the hPN end-blocks. [c] Following deformation to 300% strain.

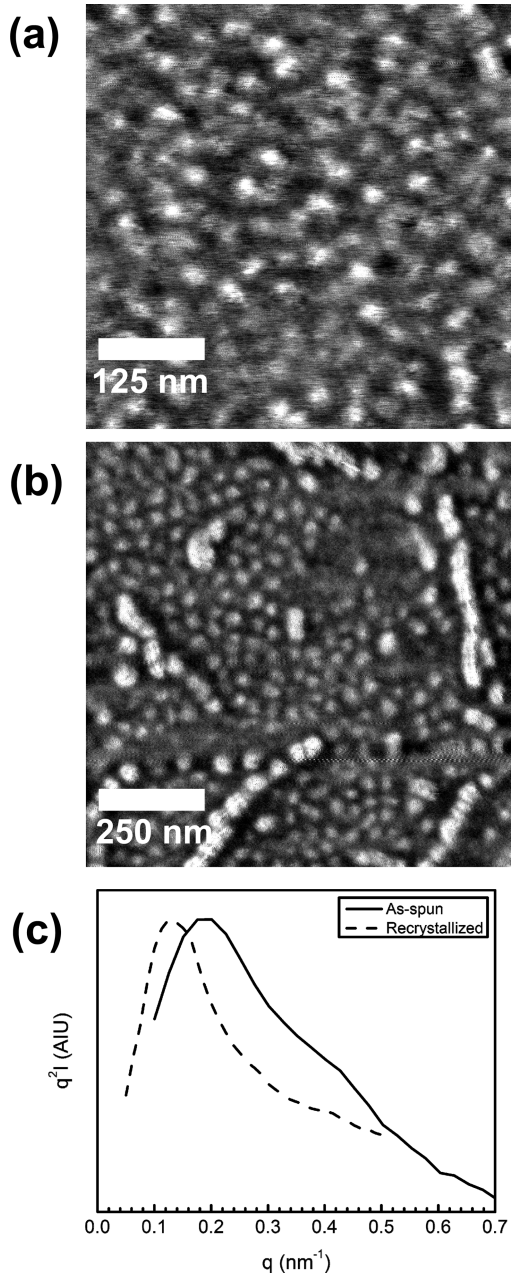

Figure 5. AFM phase images of pentablock-14 (a) immediately after spin-coating and (b) after heating into the melt and isothermally recrystallizing at 65 °C. (c) Fourier transforms of the images shown in (a) and (b).

pattern in Figure 4b.) However, it is well-known that block copolymers crystallized from solution can exhibit very different morphologies than when crystallized from the melt.[32] Consequently, the spin-coated film was subsequently heated into the melt at 140 °C, then cooled to 65 °C, and held for 90 min to isothermally crystallize the specimen. The AFM image of the isothermally crystallized film is shown in Figure 5b. The nodular structure evident in Figure 5a is again present, along with some linear "pearl necklace" features. We interpret these linear features to reflect more extended growth of the hPN crystals during isothermal crystallization, though they are still of rather limited length (and very limited width), with a nodular structure present along their length. Thus, the hard domains in pentablock-14 remain substantially discontinuous even when the material is crystallized isothermally; the peak position ($q^* = 0.13$ nm^{-1}) in the Fourier transform (Figure 5c) of the image of the isothermally

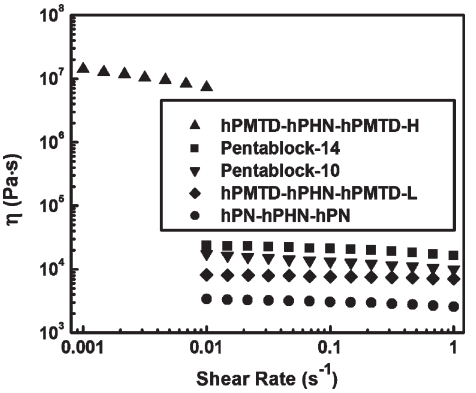

Figure 6. Steady-shear viscosity−shear rate curves at 180 °C for the ROMP TPEs.

crystallized sample is in general agreement with the peak position ($q^* = 0.104$ nm^{-1}) measured by SAXS on a bulk specimen (Figure 4b).

Confirmation of these polymers' melt states (homogeneous vs microphase-separated) was also obtained by rheometry. As shown in Figure 6, the viscosity−shear rate curves for both pentablocks as well as hPN−hPHN−hPN and the lower-molecular-weight hPMTD−hPHN−hPMTD-L all show viscosities at 180 °C on the order of 10^4 Pa·s, with weak shear-thinning behavior. The modest viscosity differences among these four polymers tracks with molecular weight; M_n ranges from 128 to 200 kg/mol among the four, all with comparably narrow distributions. By contrast, hPMTD−hPHN−hPMTD-H shows a melt viscosity some 3 orders of magnitude higher (despite having only a slightly higher M_n = 250 kg/mol) and shows shear-thinning behavior even at shear rates as low as 10^{-3} s^{-1}. The high viscosity of hPMTD−hPHN−hPMTD-H reflects its microphase-separated structure and the high segmental friction within hPMTD-rich domains at 180 °C (hPMTD homopolymer T_g = 163 °C). Moreover, the hPMTD−hPHN−hPMTD-H melt was too elastic to even load into the cone-and-plate fixture used to test the other four polymers—the normal stresses did not relax on a reasonable time scale. Similar results were obtained at 200 °C (see Supporting Information). These observations confirm the microphase-separated nature of hPMTD−hPHN−hPMTD-H in the melt, and the homogeneous state of the other four polymers, including both pentablocks.

Turning now to the solid-state properties of these materials, DSC was used to determine (Table 2) the rubbery domain T_g and the melting point and degree of crystallinity in the polymers containing hPN. Both pentablocks, as well as hPN−hPHN−hPN and hPMTD−hPHN−hPMTD-H, all show rubbery-domain glass transition temperatures that are only slightly above that of the homopolymer hPHN[20] (−22 °C), indicating good microphase separation between the rubbery and hard components, as expected from the SAXS patterns in Figures 2 and 4. In particular, this simple DSC measurement on the two pentablocks shows that the hPMTD blocks are well segregated from their neighboring hPHN blocks in the solid, even though all blocks are homogeneously mixed in the melt. As noted previously, pentablock-10 has a very low degree of crystallinity of the hPN endblocks, just 15%. This low degree of crystallinity results in a polymer with essentially no solvent resistance, as the polymer can be completely dissolved at room temperature in cyclohexane. Pentablock-14, which has shorter hPMTD blocks, has a much higher degree of crystallinity than pentablock-10, matching the hPN block crystallinity in hPN−hPHN−hPN. Pentablock-14 and hPN−hPHN−hPN do not dissolve at room temperature in any of the organic solvents tested—cyclohexane, THF, and

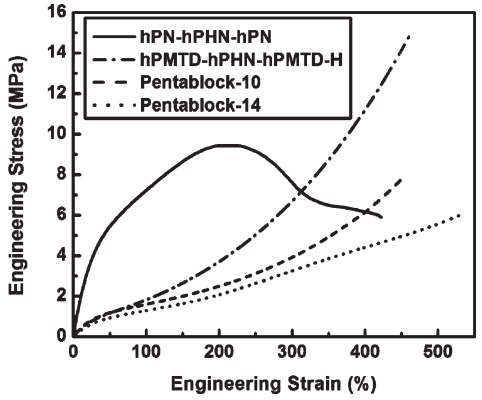

Figure 7. Uniaxial stress−strain curves for the ROMP TPEs.

toluene—though both polymers swell extensively due to their relatively low crystalline block contents.

Uniaxial stress−strain curves of the hydrogenated ROMP TPEs are shown in Figure 7, with Table 2 listing values of Young's modulus (E), tensile strength (σ_u), engineering strain at break (ε_b), and permanent set following deformation to 300% engineering strain. hPMTD−hPHN−hPMTD-H shows the typical stress−strain curve for a good elastomer—low initial modulus (4.2 MPa), no obvious yield point, and strain-hardening at higher deformations—and also shows a modest permanent set (8%). All of these are consistent with the glassy, cylindrical hard domains in hPMTD−hPHN−hPMTD-H; for comparison, the measured plateau modulus of hPHN homopolymer[20] yields a Young's modulus of 1.1 MPa, so the hard domains in hPMTD−hPHN−hPMTD-H raise the modulus roughly 4-fold. By contrast, hPN−hPHN−hPN—which has only crystalline hard domains—shows a high initial modulus (22 MPa), plastic deformation of the hard crystalline domains at only moderate strains, and a substantial permanent set (44%), reflecting a polymer with poor elastomeric properties. All of these qualities are consistent with the alternating lamellar structure of hPN−hPHN−hPN, wherein the crystalline hPN hard domains are initially platelike crystals of large lateral extent (producing the high modulus); while these crystals yield and fragment at modest strains, the fragments can subsequently fuse with fragments which originated in other crystals, producing new, stable crystals and leading to the substantial permanent set.[23] These two materials thus represent the extremes of behavior we hope to capture in the pentablocks: the solid-state mechanical properties of hPMTD−hPHN−hPMTD-H, with the ease of processing of hPN−hPHN−hPN.

Indeed, both pentablocks show a low initial modulus (~4 MPa), no clear yield point, and modest permanent sets, all quite similar to hPMTD−hPHN−hPMTD-H. They also show strain-hardening behavior, though to a lesser degree than hPMTD−hPHN−hPMTD-H. This is perhaps due to the much higher tensile strength of hPMTD (56 MPa) than hPN (15 MPa); stress−strain curves for both homopolymers are provided in the Supporting Information. The low initial modulus in the pentablocks indicates that incorporating the glassy hPMTD blocks into the polymer limits the lateral growth of the hPN crystals and produces discontinuous hard domains. Indeed, the pentablocks remain optically transparent when crystallized, unlike hPN−hPHN−hPN, which becomes cloudy due to the formation of spherulites. We infer that this crystal growth restriction in the pentablocks is the consequence of the formation of a glassy hPMTD layer immediately adjacent to the hPN crystallites, which impedes the growth of crystalline lamellae. This scenario is illustrated schematically in Figure 8. Recall that the crystallization temperatures (< 70 °C) are far below the T_g for hPMTD homopolymer, so that concentration of hPMTD blocks near the crystal surfaces can

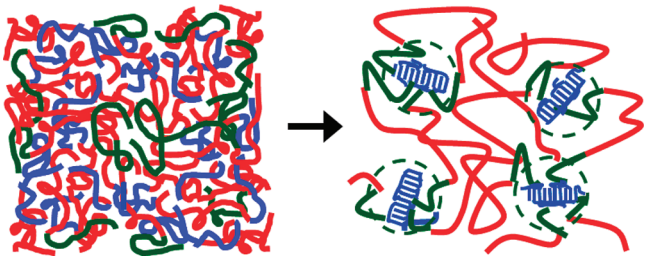

Figure 8. Schematic of the microphase-separation process in the ROMP TPE pentablocks. Crystallizable hPN blocks shown in blue; glassy hPMTD blocks shown in green; rubbery hPHN blocks shown in red. Pentablock architecture is hPN−hPMTD−hPHN−hPMTD−hPN. Left: homogeneous (single-phase) melt, where blocks are intimately mixed. Right: solid-state structure, where hPN crystallites (blue) are surrounded by glassy hPMTD layers (green), which limit the growth of the crystallites and create discontinuous composite crystalline−glassy hard domains in the rubbery hPHN matrix (red).

easily lead to vitrification. In the case of pentablock-10, where the hPN and hPMTD blocks are of equal length, this restriction is evidently quite severe, leading to a low degree of hPN crystallinity and negligible solvent resistance for the polymer. By contrast, shortening the hPMTD block and lengthening the hPN block, as in pentablock-14, produces a material where the hPN blocks can achieve a substantial degree of crystallinity but are still restricted in their lateral growth.

The excellent strain recovery of these pentablocks is noteworthy, especially among polymers where microphase separation is driven by crystallization. Pentablock-10 and pentablock-14 showed permanent sets of 9% and 6%, respectively, following 300% deformation; these values compare favorably to those for multiblock copolymers of polyethylene and poly(ethylene-*stat*-octene) at comparable hard block contents;[9,10] they surpass the recovery performance (after 300% deformation) found by Myers and Register for analogous triblock copolymers with linear polyethylene end-blocks (LPE) and an hPHN mid-block,[23] as well as that for the triblock and pentablock copolymers of isotactic polypropylene and regioirregular polypropylene examined by Hotta et al.[7] Indeed, the pentablocks presented in this work demonstrate excellent recovery for strains all the way up to the point of rupture. Pentablock-14, which has a breaking strain of 520%, showed only 10% permanent set (less than 2% of the applied strain) after rupture—slightly better than hPMTD−hPHN−hPMTD-H, where an 11% permanent set was measured following a breaking strain of 460%. The recovery performance also compares favorably with that for Kraton G1652, a commercial triblock TPE with glassy polystyrene end-blocks and a rubbery hydrogenated medium-vinyl polybutadiene (PEB) midblock (29 wt % polystyrene), which shows 5% permanent set after 300% strain and 10% permanent set after a breaking strain of 520%. These permanent set data indicate that incorporating the glassy component into the pentablocks, adjacent to the crystallizing end-blocks, establishes a robust microdomain structure in the solid state—containing composite crystalline−glassy hard domains—which is able to both sustain and recover from large deformations.

Conclusions

Symmetric pentablock copolymers having the architecture crystalline−glassy−rubbery−glassy−crystalline were synthesized by living ROMP and subsequent catalytic hydrogenation, and their performance as TPEs was compared to symmetric triblock copolymers having the architecture crystalline−rubbery−crystalline (hPN−hPHN−hPN) and glassy−rubbery−glassy (hPMTD−hPHN−hPMTD) made using the same polymerization chemistry. The total hard block content (glassy + crystalline) was held

constant at 20 wt % for consistency. The block lengths of the semicrystalline TPEs (pentablocks and hPN−hPHN−hPN) were kept low enough for their melts to be homogeneously mixed, allowing crystallization alone to drive the microphase separation needed for physical cross-linking. The hPN−hPHN−hPN triblock showed yielding of the crystalline domains at only moderate strains, resulting in a poor elastomer with high permanent set. By contrast, the pentablock copolymers showed low moduli, strain-hardening behavior, and low permanent set typical of conventional TPEs with a glassy−rubbery−glassy architecture. These differences reflect the formation of a glassy hPMTD layer surrounding the hPN crystallites, producing discontinuous hard domains which benefit from the tensile strength of glassy hPMTD. A 1:1 ratio of hPN:hPMTD produced a polymer (pentablock-10) with a low degree of crystallinity and essentially no solvent resistance, while a 2:1 ratio of hPN:hPMTD produced a polymer (pentablock-14) with good hPN block crystallinity, which prevented its dissolution at room temperature. This general approach—combining crystalline, glassy, and rubbery blocks in a pentablock architecture—should be generalizable to other monomer types and polymerization chemistries, as a way to produce TPEs with easily processed single-phase melts and a resilient crystallization-driven solid-state microdomain structure.

Acknowledgment. The authors gratefully acknowledge the National Science Foundation (Polymers Program, DMR-0505940 and -1003942) for funding. The authors gratefully acknowledge Andrew Marencic for assistance with the AFM imaging and the rheological measurements and Dr. Andrew Bell of Promerus LLC for providing the HN and MTD monomers.

Supporting Information Available: NMR spectra of the MTD monomer, and representative unsaturated block copolymers; stress−strain curves for hPMTD and hPN homopolymers and for hPMTD−hPHN−hPMTD-L; viscosity−shear rate curves for all TPEs at 200 °C. This material is available free of charge via the Internet at http://pubs.acs.org.

References and Notes

(1) Holden, G.; Bishop, E. T.; Legge, N. R. *J. Polym. Sci., Part C: Polym. Symp.* **1969**, *26*, 37–57.
(2) Ghijsels, A.; Raadsen, J. *Pure Appl. Chem.* **1980**, *52*, 1359–1386.
(3) Morton, M. *Rubber Chem. Technol.* **1983**, *56*, 1096–1110.
(4) Morton, M.; Lee, N.-C.; Terrill, E. R. In *Elastomers and Rubber Elasticity*; Mark, J. E., Lal, J., Eds.; American Chemical Society: New York, 1982; pp 101−118.
(5) Seguela, R.; Prud'homme, J. *Polymer* **1989**, *30*, 1446–1455.
(6) Mohajer, Y.; Wilkes, G. L.; Wang, I. C.; McGrath, J. E. *Polymer* **1982**, *23*, 1523–1535.
(7) Hotta, A.; Cochran, E.; Ruokolainen, J.; Khanna, V.; Fredrickson, G. H.; Kramer, E. J.; Shin, Y. W.; Shimizu, F.; Cherian, A. E.; Hustad, P. D.; Rose, J. M.; Coates, G. W. *Proc. Natl. Acad. Sci. U. S.A.* **2006**, *103*, 15327–15332.
(8) Koo, C. M.; Hillmyer, M. A.; Bates, F. S. *Macromolecules* **2006**, *39*, 667–677.
(9) Wang, H. P.; Khariwala, D. U.; Cheung, W.; Chum, S. P.; Hiltner, A.; Baer, E. *Macromolecules* **2007**, *40*, 2852–2862.
(10) Wang, H. P.; Chum, S. P.; Hiltner, A.; Baer, E. *J. Polym. Sci., Part B: Polym. Phys.* **2009**, *47*, 1313–1330.
(11) Arriola, D. J.; Carnahan, E. M.; Hustad, P. D.; Kuhlman, R. L.; Wenzel, T. T. *Science* **2006**, *312*, 714–719.
(12) Adams, R. K.; Hoeschele, G. K.; Witsiepe, W. K. In *Thermoplastic Elastomers*, 2nd ed.; Holden, G., Legge, N. R., Quirk, R. P., Schroeder, H. E., Eds.; Hanser/Gardner Publications: Cincinnati, 1996; pp 192−225.
(13) Veenstra, H.; Hoogvliet, R. M.; Norder, B.; de Boer, A. P. *J. Polym. Sci., Part B: Polym. Phys.* **1998**, *36*, 1795–1804.
(14) Falk, J. C.; Schlott, R. J. *Angew. Makromol. Chem.* **1972**, *21*, 17–23.
(15) Park, C.; De Rosa, C.; Fetters, L. J.; Thomas, E. L. *Macromolecules* **2000**, *33*, 7931–7938.
(16) Schmalz, H.; Böker, A.; Lange, R.; Krausch, G.; Abetz, V. *Macromolecules* **2001**, *34*, 8720–8729.
(17) Mahanthappa, M. K.; Lim, L. S.; Hillmyer, M. A.; Bates, F. S. *Macromolecules* **2007**, *40*, 1585–1593.
(18) Mahanthappa, M. K.; Hillmyer, M. A.; Bates, F. S. *Macromolecules* **2008**, *41*, 1341–1351.
(19) Fleury, G.; Bates, F. S. *Macromolecules* **2009**, *42*, 3598–3610.
(20) Hatjopoulos, J. D.; Register, R. A. *Macromolecules* **2005**, *38*, 10320–10322.
(21) Asrar, J.; Curran, S. A. *J. Mol. Catal.* **1991**, *65*, 1–14.
(22) Dounis, P.; Feast, W. J. *Polymer* **1996**, *37*, 2547–2554.
(23) Myers, S. B.; Register, R. A. *Macromolecules* **2009**, *42*, 6665–6670.
(24) Sebastian, J. M.; Register, R. A. *J. Appl. Polym. Sci.* **2001**, *82*, 2056–2069.
(25) Lee, L.-B. W.; Register, R. A. *Macromolecules* **2004**, *37*, 7278–7284.
(26) Register, R. A.; Bell, T. R. *J. Polym. Sci., Part B: Polym. Phys.* **1992**, *30*, 569–575.
(27) Huang, T. C.; Toraya, H.; Blanton, T. N.; Wu, Y. *J. Appl. Crystallogr.* **1993**, *26*, 180–184.
(28) Lee, L. B. W.; Register, R. A. *Macromolecules* **2005**, *38*, 1216–1222.
(29) Sohn, B. H.; Gratt, J. A.; Lee, I. K.; Cohen, R. E. *J. Appl. Polym. Sci.* **1995**, *58*, 1041–1046.
(30) Hashimoto, T.; Kawamura, T.; Harada, M.; Tanaka, H. *Macromolecules* **1994**, *27*, 3063–3072.
(31) Lee, L. B. W. Ph.D. Thesis, Princeton University, **2004**.
(32) Cohen, R. E.; Cheng, P. L.; Douzinas, K.; Kofinas, P.; Berney, C. V. *Macromolecules* **1990**, *23*, 324–327.